Supplementary Information

Fabrication of Super-Lubricous Polyethylene Glycol Hydrogel Microspheres

Samuel Stealey[1], Ether Dharmesh[1], Maitreyi Bhagat[2], Abdul Malik Tyagi[3], Andrew Schab[1], Melissa Hong[2], Damon Osbourn[2], Yousef Abu-Amer[3], Paul A. Jelliss[2], Silviya Petrova Zustiak[1,*]

[1] Department of Biomedical Engineering, School of Science and Engineering, Saint Louis University, Saint Louis, MO

[2] Department of Chemistry, School of Science and Engineering, Saint Louis University, Saint Louis, MO

[3] Department of Orthopaedics, Washington University in Saint Louis, Saint Louis, MO

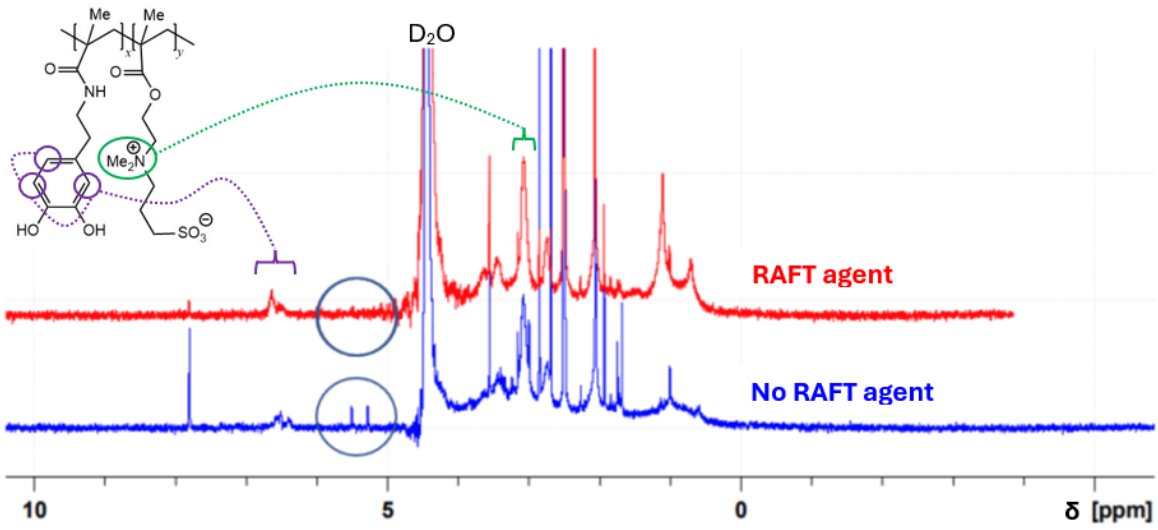

Supplementary Figure 1. 400 MHz NMR spectra of poly(DMA-co-SBMA) in PBS/D_2O. Products recovered by dialysis after polymerization with and without RAFT agent.

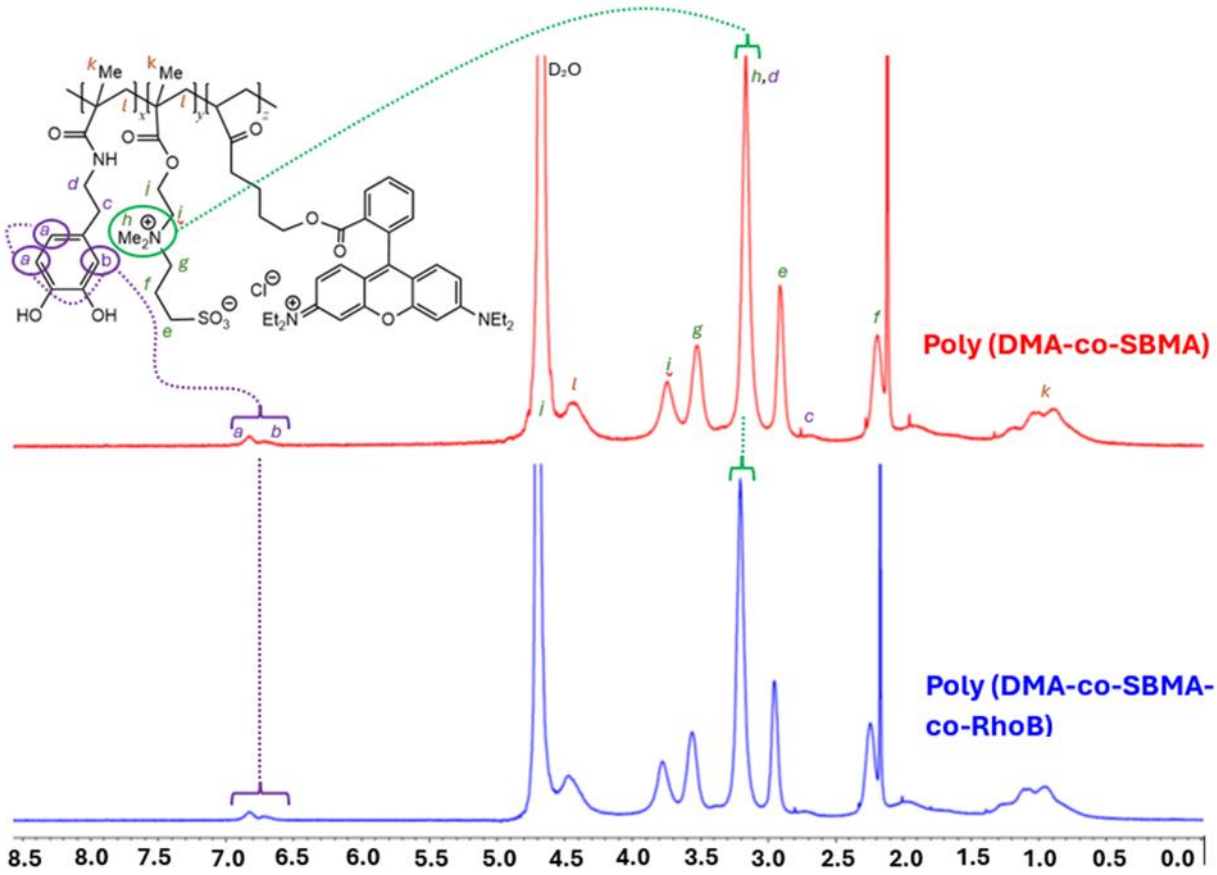

Supplementary Figure 2. 400 MHz NMR spectra of poly(DMA-co-SBMA) and poly(DMA-co-SBMA-co-RhoB) in PBS/D_2O. Chemical shift assignments for DMA and SBMA residues are shown in the top spectrum. DMA (purple): δ 6.82 [2H, Ph(*a*)], 6.73 [1H, Ph(*b*)], 3.20 [2H, CH_2(*d*)], 2.72 [2H, CH_2(*c*)]; SBMA (green): δ 4.46 [2H, CH_2(*j*)+D_2O], 3.77 [2H, CH_2(*i*)], 3.56 [2H, CH_2(*g*)], 3.20 [6H, NMe_2(*h*)], 2.94 [2H, CH_2(*e*)], 2.24 [2H, CH_2(*f*)]; polymer backbone (brown): 4.47 [2H, CH_2(*l*)], 1.00 [3H, Me(*k*)].

Supplementary Figure 3. Macroscopic photograph of poly(DMA-co-SBMA) (**Left**) and poly(DMA-co-SBMA-co-RhoB) (**Right**), with the pinkish color being attributed to the incorporation of RhoB within the copolymer.

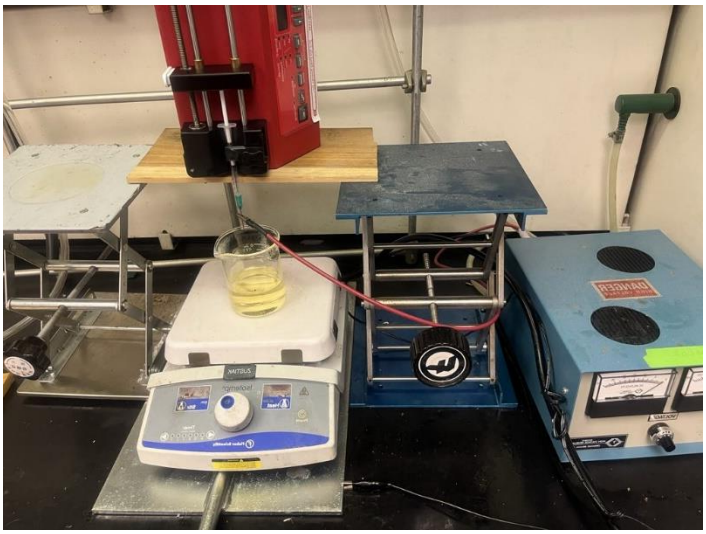

Supplementary Figure 4. Photograph of Electrospraying Setup. PEG is loaded into a syringe with attached blunt tip needle, which is then mounted on a programmable syringe pump. The syringe needle tip is attached via clip to a high voltage generator. The oil collection vessel is mounted on a stir plate on top of a grounded metal sheet. Stirring rate is programmed with stir plate and stir bar within oil collection vessel.

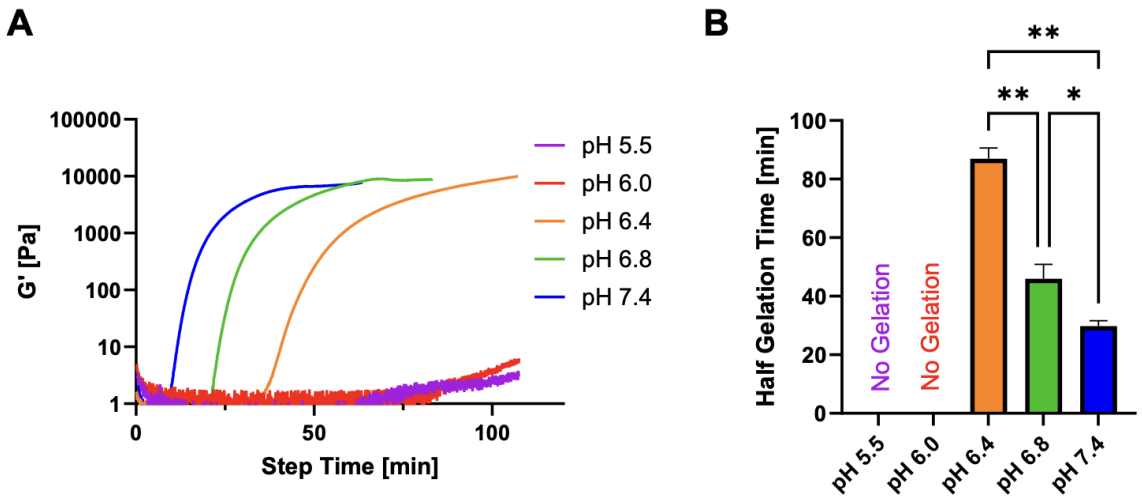

Supplementary Figure 5: Gelation kinetics (**A**) and calculated half-gelation time (**B**) of 4-arm PEG-Ac and PEG-diSH at varying pH. Gelation kinetics were measured via rheology, where increase in polymer solution storage modulus, G', was indicative of gelation. * indicates $p < 0.05$, while ** indicates $p < 0.01$ ($N = 4$).

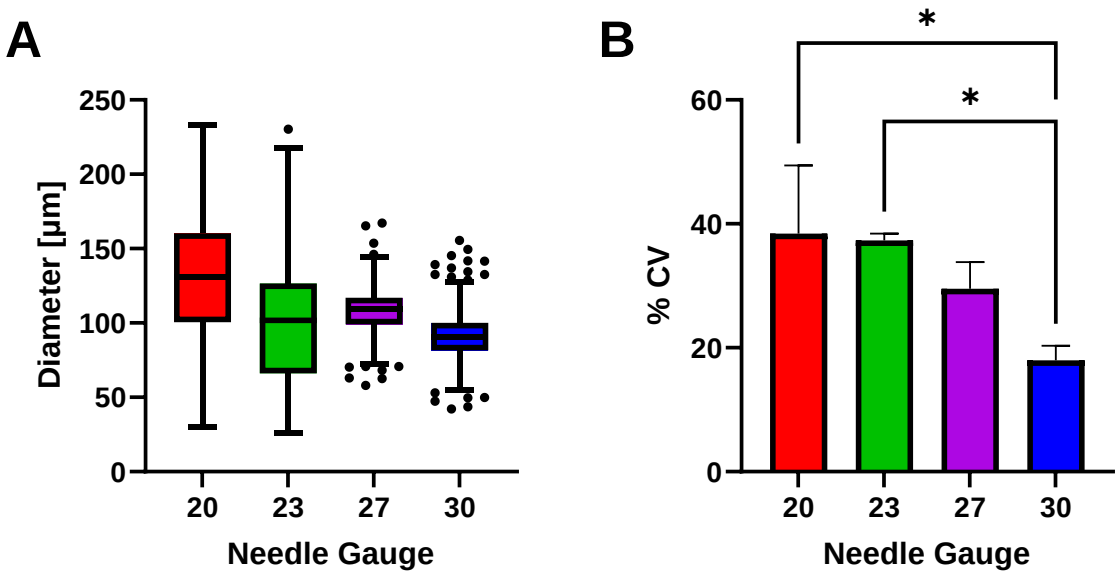

Supplementary Figure 6: A. Distribution of droplet diameters following electrospraying with varying needle diameter. **B.** Polydispersity of droplet diameters following electrospraying with varying needle diameter. * indicates statistically significant difference ($N = 3$, $p < 0.05$).

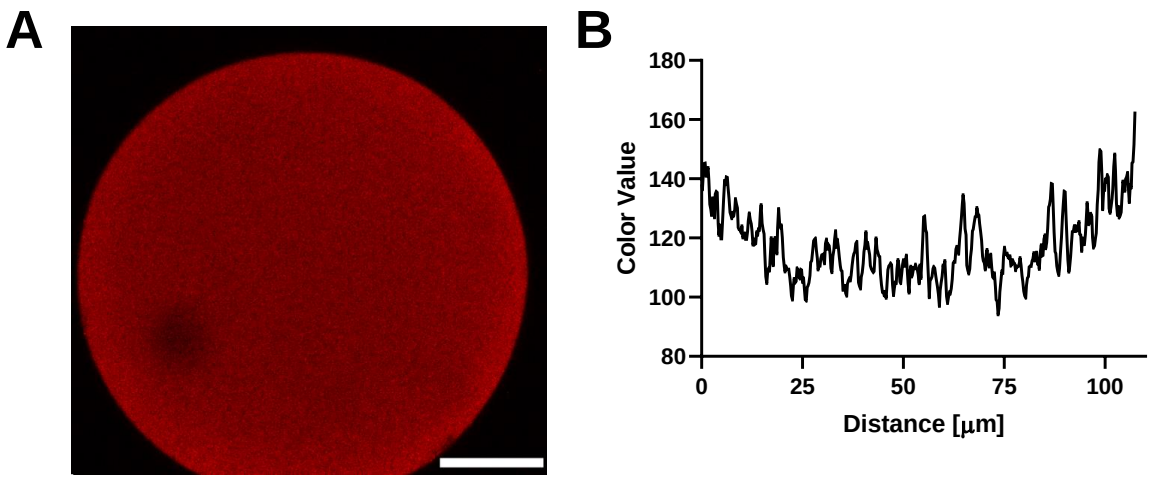

Supplementary Figure 7: A. Confocal slice of poly(DMA-co-SBMA-co-RhoB)-coated PEG microsphere. Scale bar represents 25 μm. **B.** Quantification of red color value from confocal image, where a color value of 0 represents no fluorescence, and a value of 255 represents the upper end of fluorescence.

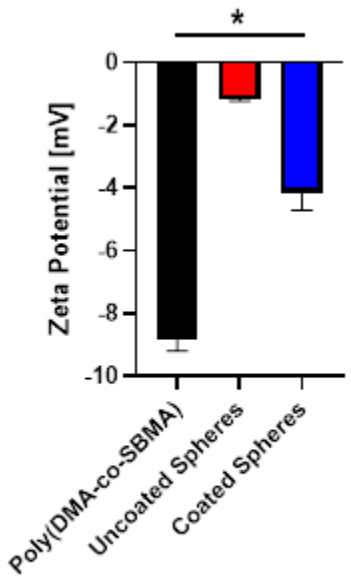

Supplementary Figure 8: Zeta potential measurements of 10 mg/mL poly(DMA-co-SBMA) and PEG microspheres without and with poly(DMA-co-SBMA) coating. * indicates statistically significant difference between all groups ($p < 0.05$, $N = 3$).

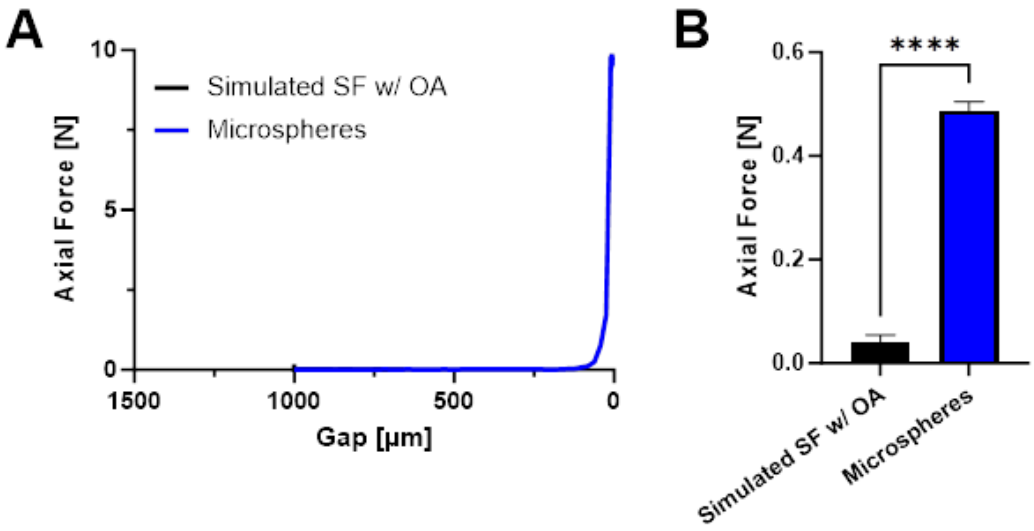

Supplementary Figure 9: A. Validation of rheological compression of hydrogel microspheres, where geometry gap was lowered and axial force recorded. **B.** Measured axial force at a gap of 10 µm.

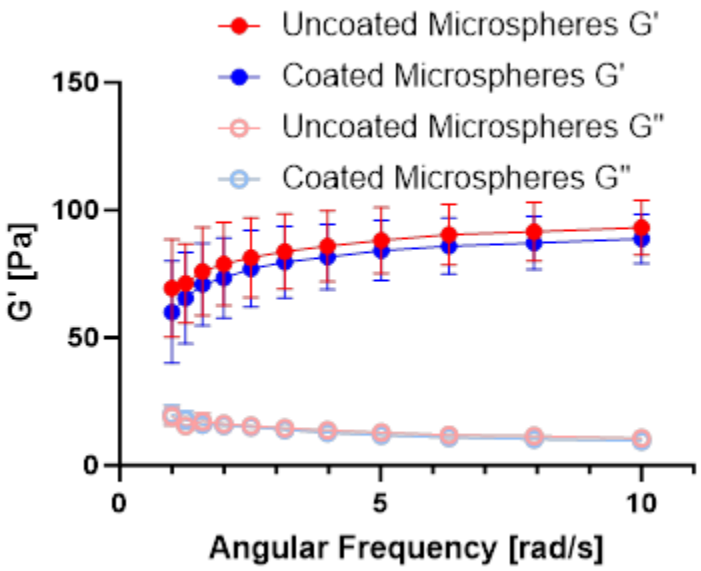

Supplementary Figure 10: Evolution of storage modulus, *G'*, and loss modulus, *G"*, as a function of angular frequency.